# Peristaltic transport of MHD Carreau fluid under the effect of partial slip with different wave forms

**M. Sukumar* and S.V.K. Varma**

**Abstract:** This article investigates with the effects of magnetic field and partial slip on the peristaltic transport of Carreau fluid with different wave form the model in an asymmetric channel has been investigated. The problem is simplified by using long wavelength and low Reynolds number approximations. The perturbation and numerical presented. The expressions for pressure rise, pressure gradient, stream function, magnetic force function, current density distribution have been computed. The results of pertinent parameters have been discussed graphically. The trapping phenomena for different wave forms have been also discussed.

**Key words:** peristaltic transport; Hartmann number; Weissenberg number; partial slip; shear stress; trapping; different wave forms.

## 1. Introduction

Peristaltic pumping has been the object of scientific and engineering research in recent years. The word peristaltic comes from a Greek word Peristaltikos which means clasping and compressing. The peristaltic transport is traveling contraction wave along a tube-like structure, and it results physiologically from neuron-muscular properties of any tubular smooth muscle. Peristaltic motion of blood in animal or human bodies has been considered by many authors. It is an important mechanism for transporting blood, where the cross-section of the artery is contracted or expanded periodically by the propagation of progressive wave. It plays an indispensable role in transporting many physiological fluids in the body in various situations such as urine transport from the kidney to the bladder through the ureter, transport of spermatozoa in the ducts efferentes of the male reproductive tract and the movement of ovum in the fallopin tubes. Some worms to make locomotion using the mechanism of peristalsis. Roller and finger pumps using viscous fluids also operate on this principle, gastro-intestinal tract, bile ducts and other glandular ducts. The principle of peristaltic transport has been exploited for industrial applications like sanitary fluid transport, blood pumps in heart lungs machine and transport of corrosive fluids where the contact of the fluid with the machinery parts is prohibited. Since the first investigation of Latham [1], extensive analytical studies have been undertaken which involve such fluids. Important studies to the topic include the works in [2–11].

Recently, MHD peristaltic flows have acquired a lot of credence due to their applications. The effects of MHD on the peristaltic flow of Newtonian and non-Newtonian fluids for different geometries have been discussed by many researchers [12–15], with a view to understand some practical phenomena such as blood pump machine and Magnetic Resonance Imaging (MRI) which is used for diagnosis of brain, vascular diseases and all the human body. In the studies [12–15], the uniform MHD has been used. There are a few attempts in which induced magnetic field is used. They are mentioned in the works of [16–25]. The flow of Carreau fluid with partial slip under the effect of magnetic field with different wave forms and yield stress on the pumping characteristics have been reported in their investigation, the assumption for the solution is that wavelength of the peristaltic wave is long. A regular perturbation technique is employed to solve the present problem and solutions are expanded in a power of small Weissenberg number. The analysis is made for the stream function, axial pressure gradient and pressure rise over a wavelength. The influence of emerging parameters is shown on pumping, pressure gradient and trapping.

M. Sukumar*****, Department of Mathematics, S.V. University, Tirupati- 517 502, India. *Corresponding author E-mail: sukumarphd@gmail.com
S. V. K. Varma, Department of Mathematics, S.V. University, Tirupati- 517 502, India. E-mail svijayakumarvarma@yahoo.co.in

## 2. Mathematical formulation

Let us consider the peristaltic transport of an incompressible Carreau fluid under the effect of magnetic field in a two–dimensional channel of width $d_1 + d_2$. The flow is generated by sinusoidal wave trains propagating with constant speed c along the asymmetric channel with partial slip. The geometry of the wall surfaces is defined as

$$h_1\left(\bar{X},\bar{t}\right)=\bar{d}_1+\bar{a}_1\cos\left[\frac{2\pi}{\lambda}\left(\bar{X}-c\bar{t}\right)\right]\cdots\cdots\cdots\cdots \text{ upper walls} \quad (1)$$

$$h_2\left(\bar{X},\bar{t}\right)=-\bar{d}_2-\bar{a}_2\cos\left[\frac{2\pi}{\lambda}\left(\bar{X}-c\bar{t}\right)+\phi\right]\cdots\cdots \text{ lower wall} \quad (2)$$

in which $\bar{a}_1$ and $\bar{a}_2$ are the amplitudes of the waves, $\lambda$ is the wave length, $c$ is the wave speed, $\phi$ $(0\le\phi\le\pi)$ is the phase difference, $\bar{X}$ and $\bar{Y}$ are the rectangular coordinates with $\bar{X}$ measured along the axis of the channel and $\bar{Y}$ is perpendicular to $\bar{X}$. Let $(\bar{U},\bar{V})$ be the velocity components in fixed frame of reference $(\bar{X},\bar{Y})$. It should be noted that $\phi=0$ it corresponds to symmetric channel with waves out of phase and for $\phi=\pi$ the waves are in phase. Furthermore, $\bar{a}_1$, $\bar{a}_2$, $\bar{d}_1$, $\bar{d}_2$ and $\phi$ satisfy the condition

$$\bar{a}_1^{\,2}+\bar{a}_2^{\,2}+2\bar{a}_1\bar{a}_2\cos\phi\le\left(\bar{d}_1+\bar{d}_2\right)^2. \quad (3)$$

## 3. Equations of motion

The constitutive equation for a Carreau fluid is

$$\bar{\tau}=-\left[\eta_\infty+\left(\eta_0-\eta_\infty\right)\left(1+\left(\Gamma\bar{\dot{\gamma}}\right)^2\right)^{\frac{n-1}{2}}\right]\bar{\dot{\gamma}}, \quad (4)$$

where $\tau$ is the extra stress tensor, $\eta_\infty$ is the infinite shear rate viscosity, $\eta_0$ is the zero shear-rate viscosity, $\Gamma$ is the time constant, $n$ is the dimensionless power law index and $\dot{\gamma}$ is defined as

$$\bar{\dot{\gamma}}=\sqrt{\frac{1}{2}\sum_i\sum_j\bar{\dot{\gamma}}_{ij}\bar{\dot{\gamma}}_{ji}}=\sqrt{\frac{1}{2}\Pi}. \quad (5)$$

here $\Pi$ is the second invariant of strain- rate tensor. We consider in the constitutive Eq. (4) the case for which $\eta_\infty=0$, and so we can write

$$\bar{\tau}=-\eta_0\left[1+\left(\Gamma\bar{\dot{\gamma}}\right)^2\right]^{\frac{n-1}{2}}\bar{\dot{\gamma}}. \quad (6)$$

The above model reduces to Newtonian Model for $n$=1 or $\Gamma=0$.

The flow is unsteady in the laboratory frame $(\bar{X},\bar{Y})$. However, if observed in a moving coordinate system with the wave speed $c$ (wave frame) $(\bar{x},\bar{y})$ it can be treated as steady. The coordinates and velocities in the two frames are

$$\bar{x}=\bar{X}-c\bar{t},\ \ \bar{y}=\bar{Y},\ \bar{u}\left(\bar{x},\bar{y}\right)=\bar{U}-c,\ \bar{v}\left(\bar{x},\bar{y}\right)=\bar{V}, \quad (7)$$

where $\bar{u}$ and $\bar{v}$ indicate the velocity components in the wave frame. The equations the following of a Carreau fluid are given by

$$\frac{\partial\bar{u}}{\partial\bar{x}}+\frac{\partial\bar{v}}{\partial\bar{y}}=0, \quad (8)$$

$$\rho\left(\bar{u}\frac{\partial}{\partial\bar{x}}+\bar{v}\frac{\partial}{\partial\bar{y}}\right)\bar{u}=-\frac{\partial\bar{p}}{\partial\bar{x}}-\frac{\partial\bar{\tau}_{\bar{x}\bar{x}}}{\partial\bar{x}}-\frac{\partial\bar{\tau}_{\bar{x}\bar{y}}}{\partial\bar{y}}-\sigma B_0\bar{u}, \quad (9)$$

$$\rho\left(\bar{u}\frac{\partial}{\partial\bar{x}}+\bar{v}\frac{\partial}{\partial\bar{y}}\right)\bar{v}=-\frac{\partial\bar{p}}{\partial\bar{y}}-\frac{\partial\bar{\tau}_{\bar{x}\bar{y}}}{\partial\bar{x}}-\frac{\partial\bar{\tau}_{\bar{y}\bar{y}}}{\partial\bar{y}}. \quad (10)$$

The following non-dimension quantities are also defined

$$x=\frac{\bar{x}}{\lambda},\ y=\frac{\bar{y}}{\bar{d}_1},\ u=\frac{\bar{u}}{c},\ v=\frac{\bar{v}}{c},\ t=\frac{c}{\lambda}\bar{t},\ h_1=\frac{\bar{h}_1}{\bar{d}_1},$$

$$h_2=\frac{\bar{h}_2}{\bar{d}_1},\tau_{xx}=\frac{\lambda}{\eta_0 c}\bar{\tau}_{\bar{x}\bar{x}},\tau_{xy}=\frac{\bar{d}_1}{\eta_0 c}\bar{\tau}_{\bar{x}\bar{y}},\tau_{yy}=\frac{\bar{d}_1}{\eta_0 c}\bar{\tau}_{\bar{y}\bar{y}},$$

$$\dot{\bar{\gamma}}=\frac{\bar{\dot{\gamma}}\bar{d}_1}{c},\ \delta=\frac{\bar{d}_1}{\lambda},\ We=\frac{\Gamma c}{d_1},\ p=\frac{\bar{d}_1^{\,2}}{c\lambda\eta_0}\bar{p},\ \mathrm{Re}=\frac{\rho c\bar{d}_1}{\eta_0},$$

$$M=\sqrt{\frac{\sigma}{\eta_0}}B_0 d_1,\ Da=\frac{k}{d_1^2},\ a=\frac{\bar{a}_1}{\bar{d}_1},b=\frac{\bar{a}_2}{\bar{d}_1},\ d=\frac{\bar{d}_2}{\bar{d}_1}. \quad (11)$$

and the stream function $\psi(x,y)$ is defined by

$$u=\frac{\partial\psi}{\partial y},\ v=-\delta\frac{\partial\psi}{\partial x}. \quad (12)$$

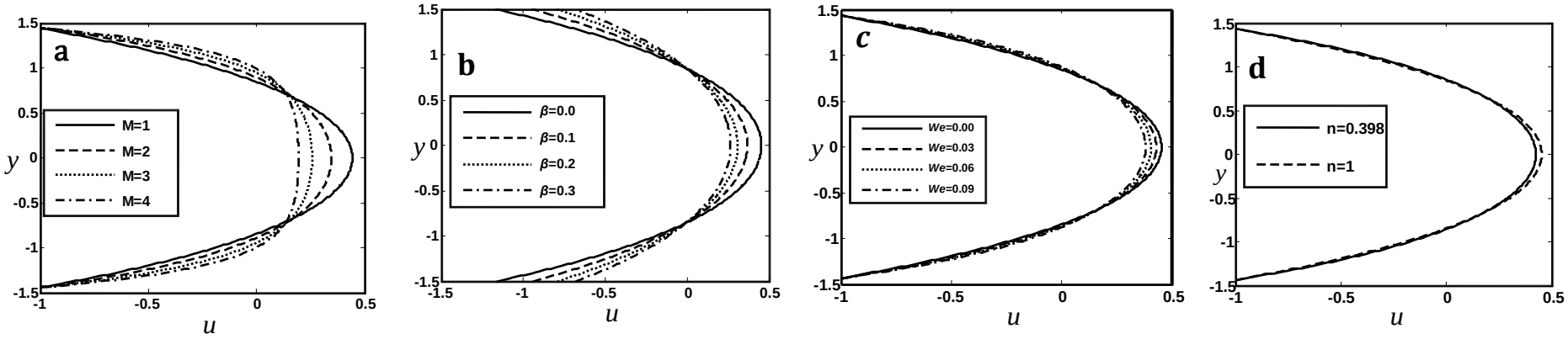


Fig. 1: The axial velocity $\boldsymbol{u}$ with $y$ for a=0.43, b=0.5, d=1, $\bar{Q}=2$ , x=1, $\phi=\pi/6$ ; (a) *We*=0.001, n=0.398, *β*=0.01; (b) *We*=0.001, n=0.398, M=1; (c) M=1, n=0.398, *β*=0.01; (d) *We*=0.001, M=1, *β*=0.01.

Using the above non-dimensional quantities have given in the Eqs. (8) - (10),

$$\delta \operatorname{Re}\left[\left(\frac{\partial\psi}{\partial y}\frac{\partial}{\partial x}-\frac{\partial\psi}{\partial x}\frac{\partial}{\partial y}\right)\frac{\partial\psi}{\partial y}\right]=-\frac{\partial p}{\partial x}-\frac{\delta^2}{2}\frac{\partial\tau_{xx}}{\partial x}-\frac{\partial\tau_{xy}}{\partial y}-M^2\frac{\partial\psi}{\partial y}, \tag{13}$$

$$-\delta^3 \operatorname{Re}\left[\left(\frac{\partial\psi}{\partial y}\frac{\partial}{\partial x}-\frac{\partial\psi}{\partial x}\frac{\partial}{\partial y}\right)\frac{\partial\psi}{\partial x}\right]=-\frac{\partial p}{\partial y}-\delta^2\frac{\partial\tau_{xy}}{\partial x}-\delta\frac{\partial\tau_{yy}}{\partial y}. \tag{14}$$

Where $$\tau_{xx}=-2\left[1+\frac{(n-1)}{2}We^2\dot{\gamma}^2\right]\frac{\partial^2\psi}{\partial x\partial y}, \tag{15}$$

$$\tau_{xy}=-\left[1+\frac{(n-1)}{2}We^2\dot{\gamma}^2\right]\left(\frac{\partial^2\psi}{\partial y^2}-\delta^2\frac{\partial^2\psi}{\partial x^2}\right), \tag{16}$$

$$\tau_{yy}=2\delta\left[1+\frac{(n-1)}{2}We^2\dot{\gamma}^2\right]\frac{\partial^2\psi}{\partial x\partial y}, \tag{17}$$

$$\dot{\gamma}=\left[2\delta^2\left(\frac{\partial^2\psi}{\partial x\partial y}\right)^2+\left(\frac{\partial^2\psi}{\partial y^2}-\delta^2\frac{\partial^2\psi}{\partial x^2}\right)+2\delta^2\left(\frac{\partial^2\psi}{\partial x\partial y}\right)^2\right]^{\frac{1}{2}}. \tag{18}$$

and $\delta$, *Re* and *We* are the wave, Reynolds and Weisssenberg numbers, respectively. Under the assumptions of long wavelength and low Reynolds number, Eqs. (13) - (14) after using Eq. (16) become

$$\frac{\partial p}{\partial x}=\frac{\partial}{\partial y}\left[1+\frac{(n-1)}{2}We^2\left(\frac{\partial^2\psi}{\partial y^2}\right)^2\right]\frac{\partial^2\psi}{\partial y^2}-M^2\frac{\partial\psi}{\partial y}, \tag{19}$$

$$\frac{\partial p}{\partial y}=0. \tag{20}$$

The pressure *p* is an eliminating from Eqs. (19)- (20), we finally get

$$\frac{\partial^2}{\partial y^2}\left[\left\{1+\frac{(n-1)}{2}We^2\left(\frac{\partial^2\psi}{\partial y^2}\right)^2\right\}\frac{\partial^2\psi}{\partial y^2}\right]-M^2\frac{\partial^2\psi}{\partial y^2}=0. \tag{21}$$

## 4. Rate of volume flow

In laboratory frame, the dimensional volume flow rate is

$$Q=\int_{\bar{h}_2(\bar{X},\bar{t})}^{\bar{h}_1(\bar{X},t)}\bar{U}\left(\bar{X},\bar{Y},\bar{t}\right)d\bar{Y}. \tag{22}$$

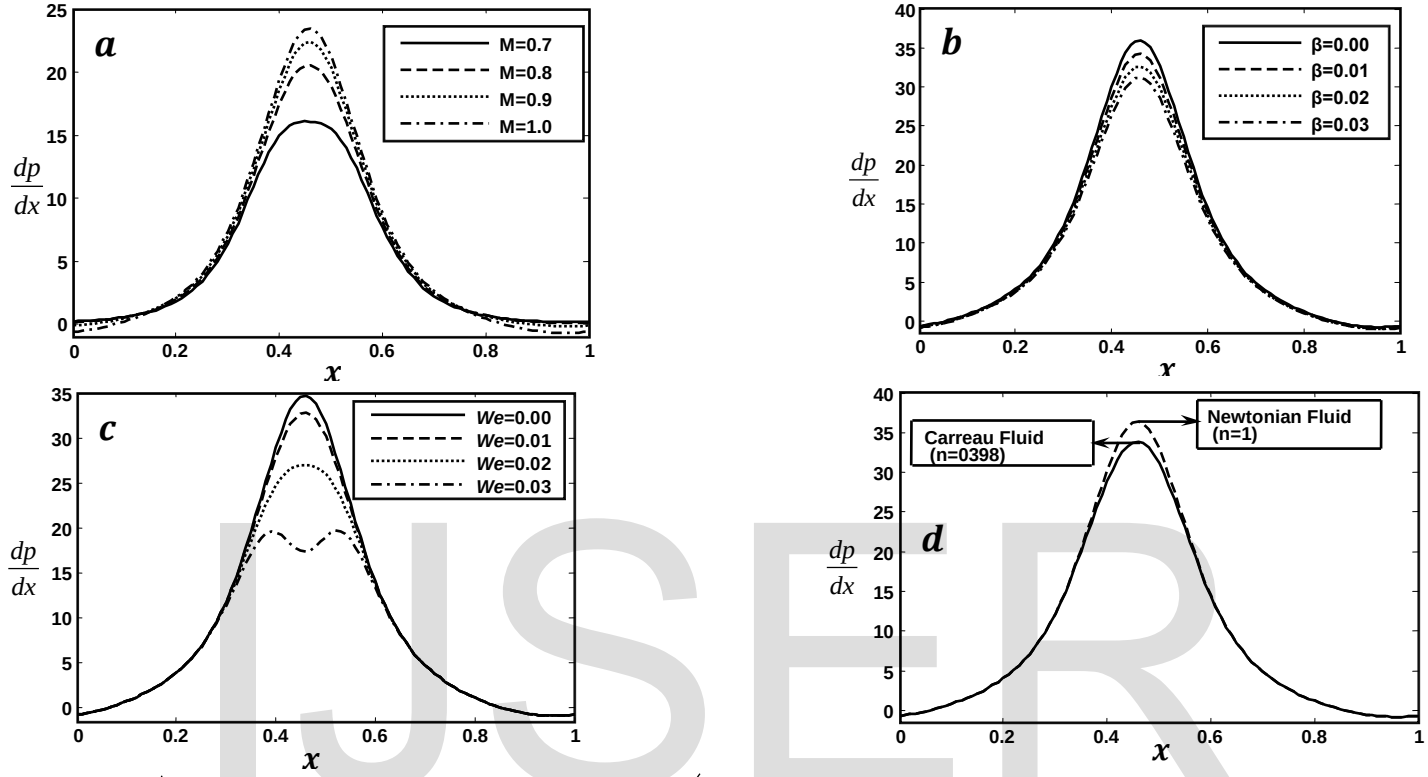


Fig. 2: The pressure distribution $dp/dx$ with $x$ for a=0.5, b=0.5, d=1, $\bar{Q}=-2$, $\phi=\pi/6$; (a) *We*=0.001, n=0.398, *β*=0.01; (b) *We*=0.001, n=0.398, M=1; (c) M=1, n=0.398, *β*=0.01; (d) *We*=0.001, M=1, *β*=0.01.

in which $\bar{h}_1$ and $\bar{h}_2$ are functions of $\bar{X}$ and $\bar{t}$, the above expression in the wave frame becomes

$$q=\int_{\bar{h}_2(\bar{x})}^{\bar{h}_1(\bar{x})}\bar{u}(\bar{x},\bar{y})d\bar{y}, \tag{23}$$

where $\bar{h}_1$ and $\bar{h}_2$ are only functions of $\bar{x}$, from Eqs. (7), (22) and (23) we can write

$$Q=q+c\bar{h}_1(\bar{x})-c\bar{h}_2(\bar{x}). \tag{24}$$

The time- averaged flow over a period *T* at a fixed position $\bar{X}$ is given as

$$\bar{Q}=\frac{1}{T}\int_0^T Qdt\cdot \tag{25}$$

where

$$\bar{Q}=\frac{\theta}{c\bar{d}_1},\quad q=\frac{F}{c\bar{d}_1}, \tag{26}$$

in which

$$F=\int_{h_2(x)}^{h1(x)}\frac{\partial\psi}{\partial y}dy=\psi\left(h_1(x)\right)-\psi\left(h_2(x)\right). \tag{27}$$

here, $h_1(x)$ and $h_2(x)$represent the dimensionless form of the surfaces of the peristaltic walls

the resulting equations in terms of stream function can be written as

$$h_1(x) = 1 + a\cos 2\pi x, \tag{28}$$

$$h_2(x) = -d - b\cos(2\pi x + \phi). \tag{29}$$

on substituting (24) into (25) and performing the integration, we obtain

$$\theta = F + c\bar{d}_1 + c\bar{d}_2, \tag{30}$$

inserting Eq. (26) into Eq. (30), yields

$$\bar{Q} = q + 1 + d. \tag{31}$$

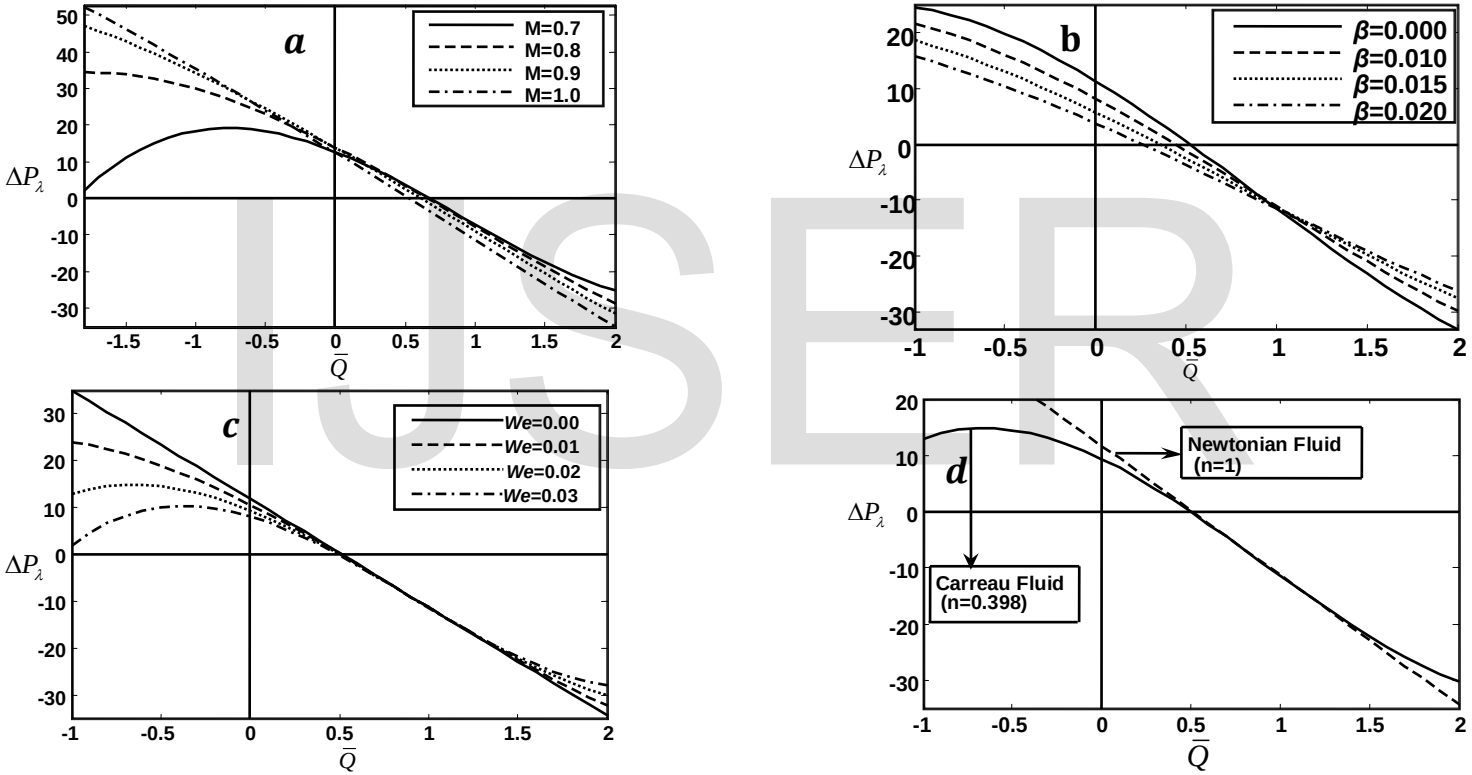


Fig. 3: The pressure rise $\Delta P_\lambda$ with $\bar{Q}$ for a=0.5, b=0.5, d=1 , $\phi = \pi/6$ ; (a) *We*=0.001, n=0.398, *β*=0.01; (b) *We*=0.001, n=0.398, M=1; (c) M=1, n=0.398, *β*=0.01; (d) *We*=0.001, M=1, *β*=0.01.

In the wave frame, the boundary conditions in terms of streams function $\psi$ are

## 5. Boundary conditions

$$\psi = \frac{q}{2} at\ y = h_1(x), \tag{32}$$

$$\psi = \frac{-q}{2} at\ y = h_2(x), \tag{33}$$

$$\frac{\partial \psi}{\partial y} + \beta \frac{\partial^2 \psi}{\partial y^2} = -1\ at\ y = h_1(x), \tag{34}$$

$$\frac{\partial \psi}{\partial y} - \beta \frac{\partial^2 \psi}{\partial y^2} = -1\ at\ y = h_2(x). \tag{35}$$

## 6. Perturbation solution

For perturbation solution, we expand $\psi$, $q$ and $p$ as

$$\psi = \psi_0 + We^2 \psi_1 + O\left(We^4\right), \tag{36}$$

$$q = q_0 + We^2 q_1 + O\left(We^4\right), \tag{37}$$

$$p = p_0 + We^2 p_1 + O\left(We^4\right). \tag{38}$$

System of order $We^0$:

$$\frac{\partial^4 \psi_0}{\partial y^4} - M^2 \frac{\partial^2 \psi_0}{\partial y^2} = 0, \tag{39}$$

$$\frac{\partial p_0}{\partial x} = \frac{\partial^3 \psi_0}{\partial y^3} - M \frac{\partial \psi_0}{\partial y}, \tag{40}$$

$$\psi_0 = \frac{q_0}{2} at\ y = h_1(x), \tag{41}$$

$$\psi_0 = \frac{-q_0}{2} at\ y = h_2(x), \tag{42}$$

$$\frac{\partial \psi_0}{\partial y} + \beta \frac{\partial^2 \psi_0}{\partial y^2} = -1\ at\ y = h_1(x), \tag{43}$$

$$\frac{\partial \psi_0}{\partial y} - \beta \frac{\partial^2 \psi_0}{\partial y^2} = -1\ at\ y = h_2(x). \tag{44}$$

System of order $We^2$

$$\frac{\partial^4 \psi_1}{\partial y^4} + \frac{(n-1)}{2} \frac{\partial^2}{\partial y^2} \left[ \left( \frac{\partial^2 \psi_0}{\partial y^2} \right)^3 \right] - M^2 \frac{\partial^2 \psi_1}{\partial y^2} = 0, \tag{45}$$

$$\frac{\partial p_1}{\partial x} = \frac{\partial^3 \psi_1}{\partial y^3} + \frac{(n-1)}{2} \frac{\partial}{\partial y} \left[ \left( \frac{\partial^2 \psi_0}{\partial y^2} \right)^3 \right] - M^2 \frac{\partial \psi_1}{\partial y}, \tag{46}$$

$$\psi_1 = \frac{q_1}{2} at\ y = h_1(x), \tag{47}$$

$$\psi_1 = \frac{-q_1}{2} at\ y = h_2(x), \tag{48}$$

$$\frac{\partial \psi_1}{\partial y} + \beta \frac{\partial^2 \psi_1}{\partial y^2} = 0\ at\ y = h_1(x), \tag{49}$$

$$\frac{\partial \psi_1}{\partial y} - \beta \frac{\partial^2 \psi_1}{\partial y^2} = 0\ at\ y = h_2(x). \tag{50}$$

### 6.1 Solution for system of order $We^0$:

Solving Eq. (39) and then using the boundary conditions given in (41) - (44) we have

$$\psi_0 = C_1 + C_2 y + C_3 \cosh My + C_4 \sinh My. \tag{51}$$

Where

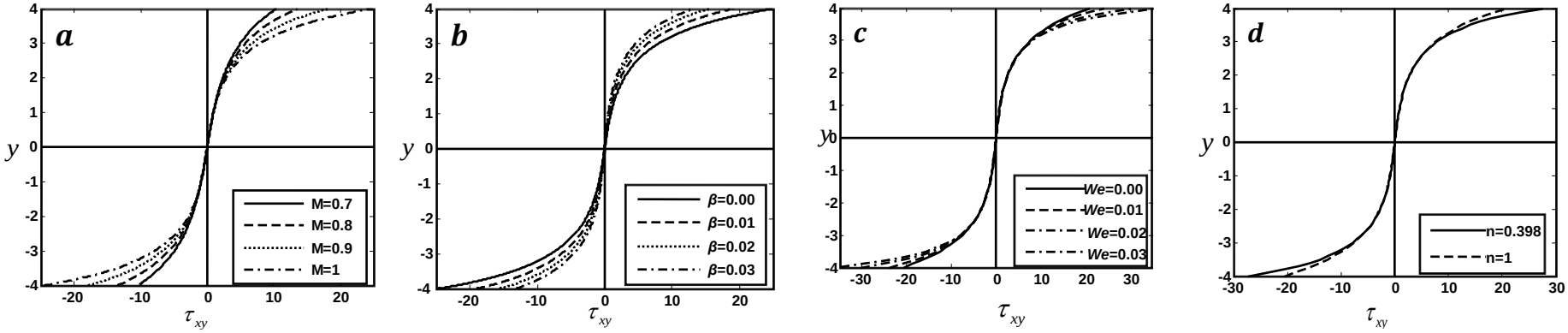


Fig. 4: The shear stress $\tau_{xy}$ with $y$ for a=0.5, b=0.5, d=1, $\bar{Q}=1.5$, x=1, $\phi=\pi/6$; (a) *We*=0.001, n=0.398, *β*=0.01; (b) *We*=0.001, n=0.398, M=1; (c) M=1, n=0.398, *β*=0.01; (d) *We*=0.001, M=1, *β*=0.01.

$$C_1=\frac{q}{2}+\frac{Mqh_1\cosh M\left(\frac{h_1-h_2}{2}\right)+\left[\left(2+M^2q\beta\right)h_1-\left(q+h_1-h_2\right)\right]\sinh M\left(\frac{h_1-h_2}{2}\right)}{\left[2-M^2\beta\left(h_1-h_2\right)\right]\sinh M\left(\frac{h_1-h_2}{2}\right)-M\left(h_1-h_2\right)\cosh M\left(\frac{h_1-h_2}{2}\right)},$$

$$C_2=-\frac{\left[\left(2+M^2q\beta\right)\sinh M\left(\frac{h_1-h_2}{2}\right)+Mq\cosh M\left(\frac{h_1-h_2}{2}\right)\right]}{\left[\left(2-M^2\beta\left(h_1-h_2\right)\right)\sinh M\left(\frac{h_1-h_2}{2}\right)\right]-M\left(h_1-h_2\right)\cosh M\left(\frac{h_1-h_2}{2}\right)},$$

$$C_3=-\frac{\left[\left(q+h_1-h_2\right)\sinh M\left(\frac{h_1+h_2}{2}\right)\right]}{\left[2-M^2\beta\left(h_1-h_2\right)\right]\sinh M\left(\frac{h_1-h_2}{2}\right)-M\left(h_1-h_2\right)\cosh M\left(\frac{h_1-h_2}{2}\right)},$$

$$C_4=\frac{\left(q+h_1-h_2\right)\cosh M\left(\frac{h_1+h_2}{2}\right)}{\left[2-M^2\beta\left(h_1-h_2\right)\right]\sinh M\left(\frac{h_1-h_2}{2}\right)-M\left(h_1-h_2\right)\cosh M\left(\frac{h_1-h_2}{2}\right)}.$$

The expressions for the axial pressure gradient at this order is

$$\frac{dp_0}{dx}=\frac{M^2\left[\left(2+M^2q\beta\right)\sinh M\left(\frac{h_1-h_2}{2}\right)+Mq\cosh M\left(\frac{h_1-h_2}{2}\right)\right]}{\left[\left(2-M^2\beta\left(h_1-h_2\right)\right)\sinh M\left(\frac{h_1-h_2}{2}\right)\right]-M\left(h_1-h_2\right)\cosh M\left(\frac{h_1-h_2}{2}\right)}. \quad (52)$$

Integrating Eq. (52) over per wavelength we get

$$\Delta P_{\lambda 0}=\int_0^1\frac{dp_0}{dx}dx. \quad (53)$$

## 6.2 Solution for system of order $We^2$

Substituting the zeroth-order solution (51) and Eq. (45) and solving the resulting system along with the corresponding boundary conditions Eqs. (47)- (50), we obtain

$$\psi_1=C_5+C_6y+C_7\cosh My+C_8\sinh My$$
$$-\frac{M^4}{64}(n-1)\left(C_3\left(C_3^2+3C_4^2\right)\cosh 3My+C_4\left(C_4^2+3C_3^2\right)\sinh 3My\right) \quad (54)$$
$$-\frac{3}{16}M^5(n-1)\left(C_3^2-C_4^3\right)\left(\left(2C_3+MC_4y\right)\cosh My+\left(MC_3y+2C_4\right)\sinh My\right).$$

where

$$C_5=\frac{q}{2}+\frac{h_1}{(h_1-h_2)}\left(\frac{qL_5}{L_7}+\frac{L_8L_5}{(h_1-h_2)L_7}+L_6-q\right)-\frac{\sinh Mh_1}{L_7}\left(\frac{q}{h_1-h_2}+L_8\right)$$
$$+\frac{\cosh Mh_1}{M(\sinh Mh_1-\sinh Mh_2)}\left(\frac{M}{L_7}(\cosh Mh_1-\cosh Mh_2)\left(\frac{q}{h_1-h_2}+L_8\right)+L_3-L_4\right)-L_1,$$

$$C_6=\frac{1}{(h_1-h_2)}\left(q-\frac{qL_5}{(h_1-h_2)L_7}-\frac{L_8L_5}{L_7}-L_6\right),$$

$$C_7=\frac{-1}{(\sinh Mh_1-\sin M\,h_2)}\left(\frac{(\cosh Mh_1-\cosh Mh_2)}{L_7}\left(\frac{q}{(h_1-h_2)}+L_8\right)+\frac{(L_3-L_4)}{M}\right),$$

$$C_8=\frac{1}{L_7}\left(\frac{q}{(h_1-h_2)}+L_8\right),$$

$$L_1=-\frac{M^4}{64}(n-1)\left(C_3\left(C_3^2+3C_4^2\right)\cosh 3Mh_1+C_4\left(C_4^2+3C_3^2\right)\sinh 3Mh_1\right)$$
$$-\frac{3}{16}M^5(n-1)h_1\left(C_3^2-C_4^2\right)\left(C_3\sinh Mh_1+C_4\cosh Mh_1\right),$$

$$L_2=-\frac{M^4}{64}(n-1)\left(C_3\left(C_3^2+3C_4^2\right)\cosh 3Mh_2+C_4\left(C_4^2+3C_3^2\right)\sinh 3Mh_2\right)$$
$$-\frac{3}{16}M^5(n-1)h_2\left(C_3^2-C_4^2\right)\left(C_3\sinh Mh_2+C_4\cosh Mh_2\right),$$

$$L_3=-\frac{3M^5(n-1)}{64}\left(\begin{array}{l}\left(C_3\left(C_3^2+3C_4^2\right)+3\beta MC_4\left(C_4^2+3C_3^2\right)\right)\sinh 3Mh_1\\+\left(C_4\left(C_4^2+3C_3^2\right)+3\beta MC_3\left(C_3^2+3C_4^2\right)\right)\end{array}\right)\cosh 3Mh_1$$
$$-\frac{3M^5(n-1)}{16}\left(C_3^2-C_4^2\right)\left(\begin{array}{l}\left(\left(C_3+Mh_1C_4\right)+3\beta M\left(Mh_1C_3+2C_4\right)\right)\sinh Mh_1\\+\left(\left(Mh_1C_3+C_4\right)+3\beta M\left(2C_3+Mh_1C_4\right)\right)\cosh Mh_1\end{array}\right),$$

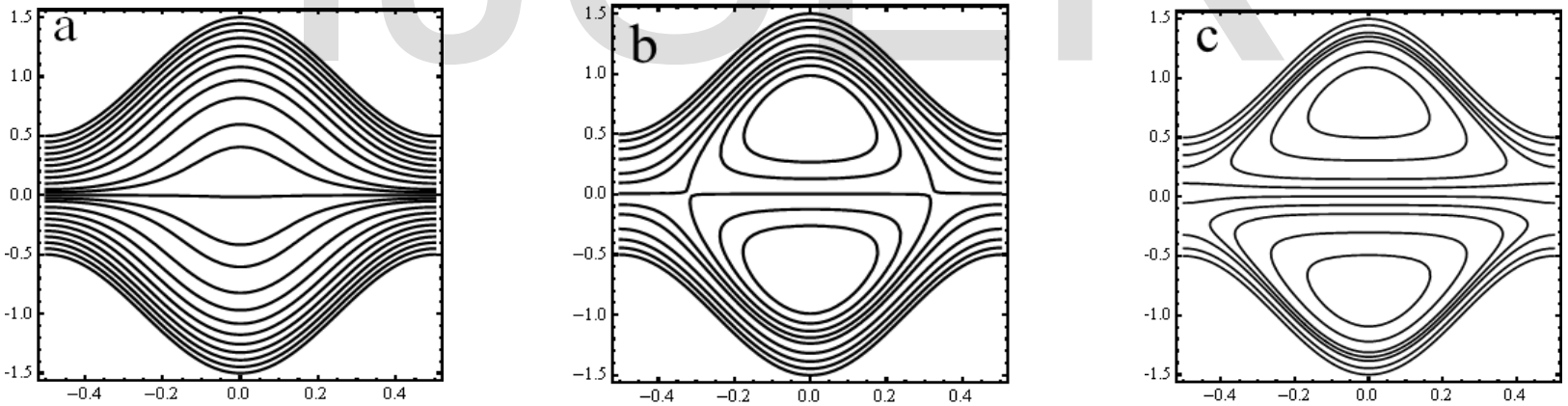


Fig. 5: The stream lines for a=0.5, b=0.5, d=1 , $\phi=0$ , *We*=0.001, n=0.398, $\beta$=0.01, M=1; (a) $\bar{Q}=1$; (b) $\bar{Q}=1.5$; (c) $\bar{Q}=2$.

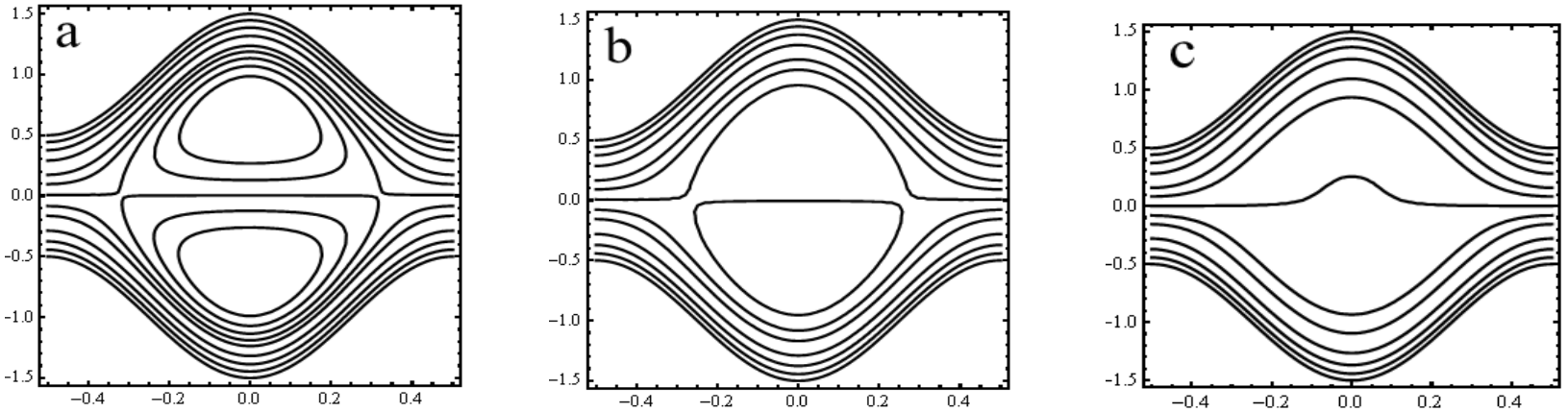


Fig. 6: The stream lines for a=0.5, b=0.5, d=1, $\bar{Q}=1.5$ , $\phi=0$ , *We*=0.001, n=0.398, $\beta$=0.01; (a) M=1; (b) M=3; (c) M=3.49.

$$L_4=-\frac{3M^5(n-1)}{64}\begin{pmatrix}\left(C_3\left(C_3^2+3C_4^2\right)+3\beta MC_4\left(C_4^2+3C_3^2\right)\right)\sinh 3Mh_2\\+\left(C_4\left(C_4^2+3C_3^2\right)+3\beta MC_3\left(C_3^2+3C_4^2\right)\right)\end{pmatrix}\cosh 3Mh_2$$

$$-\frac{3M^5(n-1)}{16}\left(C_3^2-C_4^2\right)\begin{pmatrix}\left(\left(C_3+Mh_1C_4\right)+3\beta M\left(Mh_1C_3+2C_4\right)\right)\sinh Mh_2\\+\left(\left(Mh_1C_3+C_4\right)+3\beta M\left(2C_3+Mh_1C_4\right)\right)\cosh Mh_2\end{pmatrix},$$

$$L_5=\frac{\left(\sinh Mh_1-\sinh Mh_2\right)^2-\left(\cosh Mh_1-\cosh Mh_2\right)^2}{\left(\sinh Mh_1-\sinh Mh_2\right)},$$

$$L_6=L_1-L_2-\frac{\left(L_3-L_4\right)\left(\cosh Mh_1-\cosh Mh_2\right)}{M\left(\sinh Mh_1-\sinh Mh_2\right)},$$

$$L_7=\frac{L_5}{\left(h_1-h_2\right)}+\frac{M\left(\cosh Mh_1-\cosh Mh_2\right)\left(\sinh Mh_1+\beta M\cosh Mh_1\right)}{\left(\sinh Mh_1-\sinh Mh_2\right)}$$

$$-M\left(\cosh Mh_1+\beta M\sinh Mh_1\right),$$

$$L_8=L_3-\frac{L_6}{\left(h_1-h_2\right)}-\frac{\left(L_3-L_4\right)\left(\sinh Mh_1+\beta M\cosh Mh_1\right)}{\left(\sinh Mh_1-\sinh Mh_2\right)},$$

The axial pressure gradient is given by

$$\frac{dp_1}{dx}=\frac{-M^2}{\left(h_1-h_2\right)}\left(q-\frac{qL_5}{\left(h_1-h_2\right)L_7}-\frac{L_8L_5}{L_7}-L_6\right). \quad (55)$$

Integrating Eq. (55) over are wavelength we get the pressure as

$$\Delta P_{\lambda 1}=\int_0^1\frac{dp_1}{dx}dx. \quad (56)$$

The perturbation series solution up to second order for stream function $\psi$ , velocity u, pressure gradient *dp/dx* and pressure rise $\Delta P_\lambda$ may be summarized as

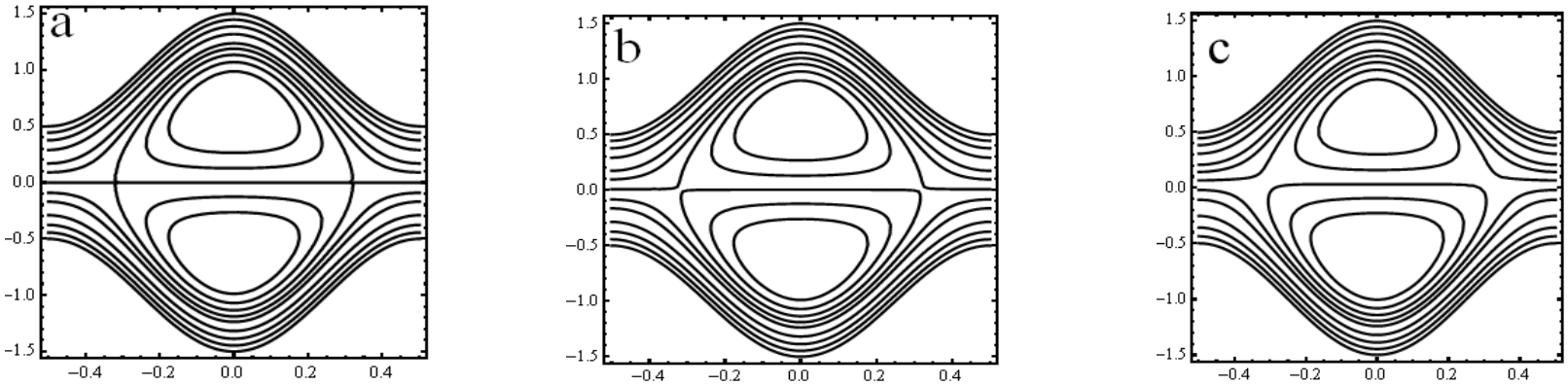


Fig. 7: The stream lines for a=0.5, b=0.5, d=1, $\bar{Q}=1.5$ , $\phi=0$ , n=0.398, $\beta$=0.01, M=1; (a) *We*=0.00; (b) *We*=0.001; (c) *We*=0.002

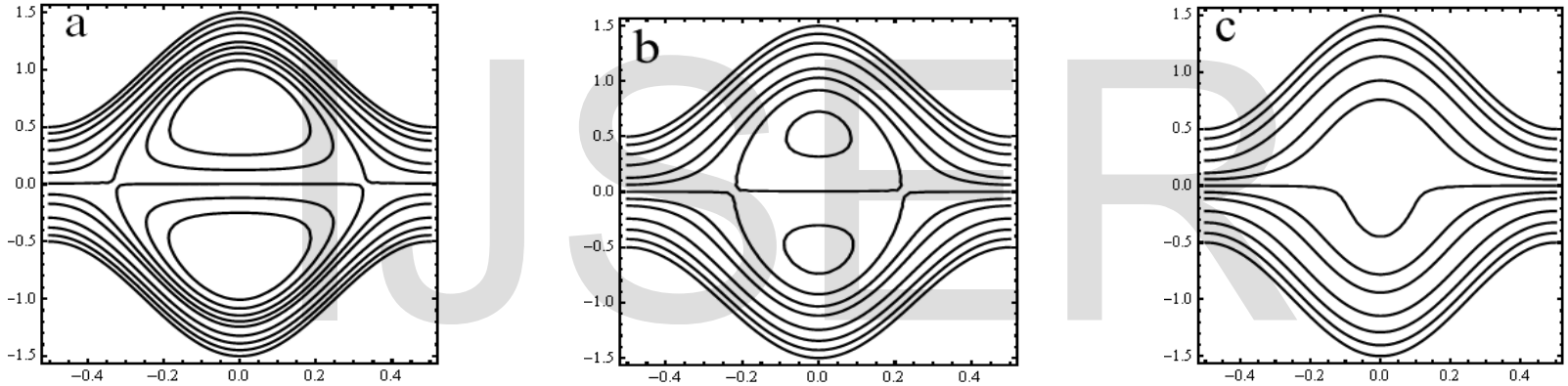


Fig. 8: The stream lines for a=0.5, b=0.5, d=1, $\bar{Q}=1.5$ , $\phi=0$ , n=0.398, M=1,*We*=0.001; (a) $\beta$=0.00; (b) $\beta$=0.025; (c) $\beta$=0.049 .

$$\psi=\psi_0+We^2\psi_1 , \tag{57}$$

$$, \frac{dp}{dx}=\frac{dp_0}{dx}+We^2\frac{dp_1}{dx} \tag{58}$$

$$\Delta P_\lambda=\Delta P_{\lambda 0}+We^2\Delta P_{\lambda 1} . \tag{59}$$

The non-dimensional shear stress of the channel reduces to

$$\tau_{xy}=-M^2C_3\cosh My-M^2C_4\sinh My-We^2\left[\frac{(n-1)}{2}\left(M^2C_3\cosh My+M^2C_4\sinh My\right)^3\right.$$
$$+M^2C_7\cosh My+M^2C_8\sinh My-\frac{9}{64}M^6(n-1)\left(\begin{matrix}C_3\left(C_3^2+3C_4^2\right)\cosh 3My\\+C_4\left(C_4^2+3C_3^2\right)\sinh 3My\end{matrix}\right) \tag{60}$$
$$\left.-\frac{3}{16}M^6(n-1)\left(C_3^2-C_4^2\right)\left(\left(2C_3+MC_4y\right)\cosh My+\left(MC_3y+2C_4\right)\sinh My\right)\right].$$

## 7. Results and discussion:

The study of the pressure rise $\bar{Q}$, velocity $u$, pressure gradient $dp/dx$ and shear stress $\tau_{xy}$ are presented and discussed for different physical quantities of interest. The pressure rise is an important physical measure in the peristaltic mechanism. The perturbation method on Weissenberg number restricted us for choosing the parameters for a Carreau fluid such that Weissenberg number is less than one. According to the values of various parameters for Carreau fluid are: n = 0.398, 0.496 and $\Gamma$=1.04, 1.58. In Figs. 1, the axial velocity distribution is shown for different parameters partial slip $\beta$, Hartmann number $M$ and Weissenberg number $(We<1)$. In Figs. 1(a)-1(c) we found that the magnitude of the axial velocity decreases in the center and increases nearer at the walls of the channel with increasing the Hartmann number $M$, partial slip $\beta$ and Weissenberg number $We$. Fig. 1(d) shows a comparison of the Carreau fluid (n=0.398) and Newtonian fluid (n=1), it is observed that the magnitude of velocity increases from Carreau fluid to Newtonian fluid. Figs.2 are plotted to see the effect of the parameters $\beta$, $M$ and $We$ on the pressure gradient $dp/dx$. Figs. 2(b) and 2(c) show that the pressure gradient $dp/dx$ decreases with increasing the partial slip $\beta$ and Weissenberg $We$, on the other hand, in the wider part of the channel $x \in [0, 0.3]$ and $x \in$ [0.6, 1] the pressure gradient is really small, that is, the flow can easily pass without imposition of a large pressure gradient. Besides, in a narrow part of the channel $x \in [0.3, 0.6]$ a much pressure gradient is required to maintain $\beta$ and $We$, it especially near $x = 0.5$. Fig. 2(a) indicates that the pressure gradient $dp/dx$ increases with increasing Hartmann number $M$ and the maximum pressure gradient is also near $x = 0.5$. Fig. 2(d) indicated that the pressure gradient in Newtonian fluid (n=1) is slightly high comparing with Carreau (n=0.398).

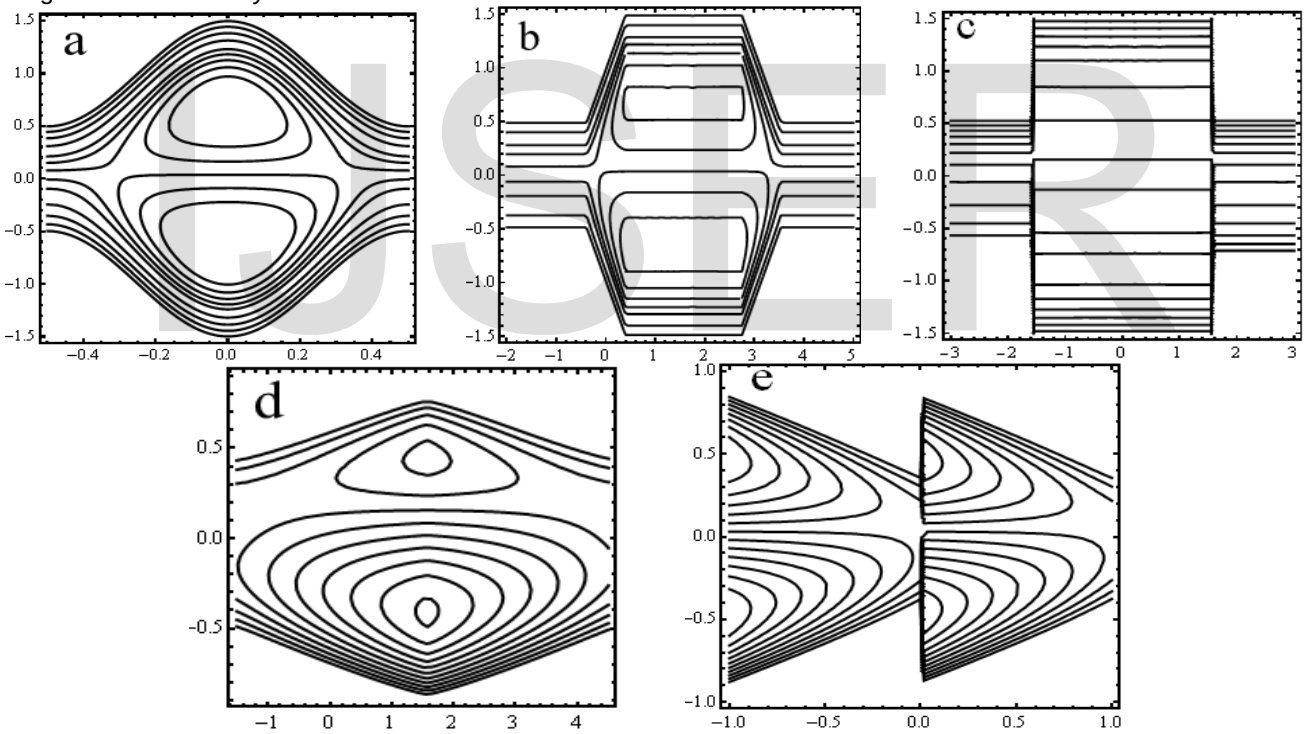


Fig. 9: The stream lines for a=0.5, b=0.5, d=1, $\bar{Q}=1.5$, $\phi=0$, n=0.398, M=1,*We*=0.001; $\beta$=0.01; (a) Sinusoidal; (b) Trapeziodal;(c) Square;(d) Triagle;(e) Sawtooth waves.

$\overline{Q} < 0$ and $\Delta P_\lambda > 0$ is called retrograde (or) backward pumping. It is shows that there is a nonlinear relation $\Delta P_\lambda$ versus $\overline{Q}$. Fig. 3(a) is a graph of the pressure rise $\Delta P_\lambda$ per wavelength versus he mean flow rate $\overline{Q}$ of the asymmetric channel for fixed values of other parameters. We observed that an increases in the Hartmann number $M$ result decrease in the peristaltic pumping rate and also in an increase in the pressure rise. Figs 3(b) and 3(c) show the variation of pressure rise $\Delta P_\lambda$ with flow rate $\overline{Q}$ for values of partial slip $\beta$ and Weissenberg number $We$ respectively. We observe that the peristaltic pumping rate decrease with increase $\beta$ and $We$. Fig. 3(d) reveals that variation of $\Delta P_\lambda$ with $\overline{Q}$ for a Carreau fluid and Newtonian fluid. It is an indicated that the Newtonian fluid peristaltic pumping rate is more than a Carreau fluid. The variation of the axial shear stress $\tau_{xy}$ with $y$ is calculated from Eq. (60) and is shown in Figs.4 for different physical parameters. In Figs. 4(a) and 4(c) we observed that the curves intersect at origin and the axial shear stress $\tau_{xy}$ decreases with increasing the Hartmann number $M$ and Weissenberg number $We$ in the upper wall and an opposite behavior is observed in the lower wall of the channel. The relation between the shear stress $\tau_{xy}$ and $y$ at different values the partial slip parameter $\beta$ is depicted in Fig. 4(b). We observe that the curves intersect at the origin and the shear stress $\tau_{xy}$ increases with increasing the partial slip parameter $\beta$ upper wall of the channel while an opposite behavior is observed in lower wall of the channel. It is observed from Fig. 4(d) that a Carreau fluid shear stress $\tau_{xy}$ is less

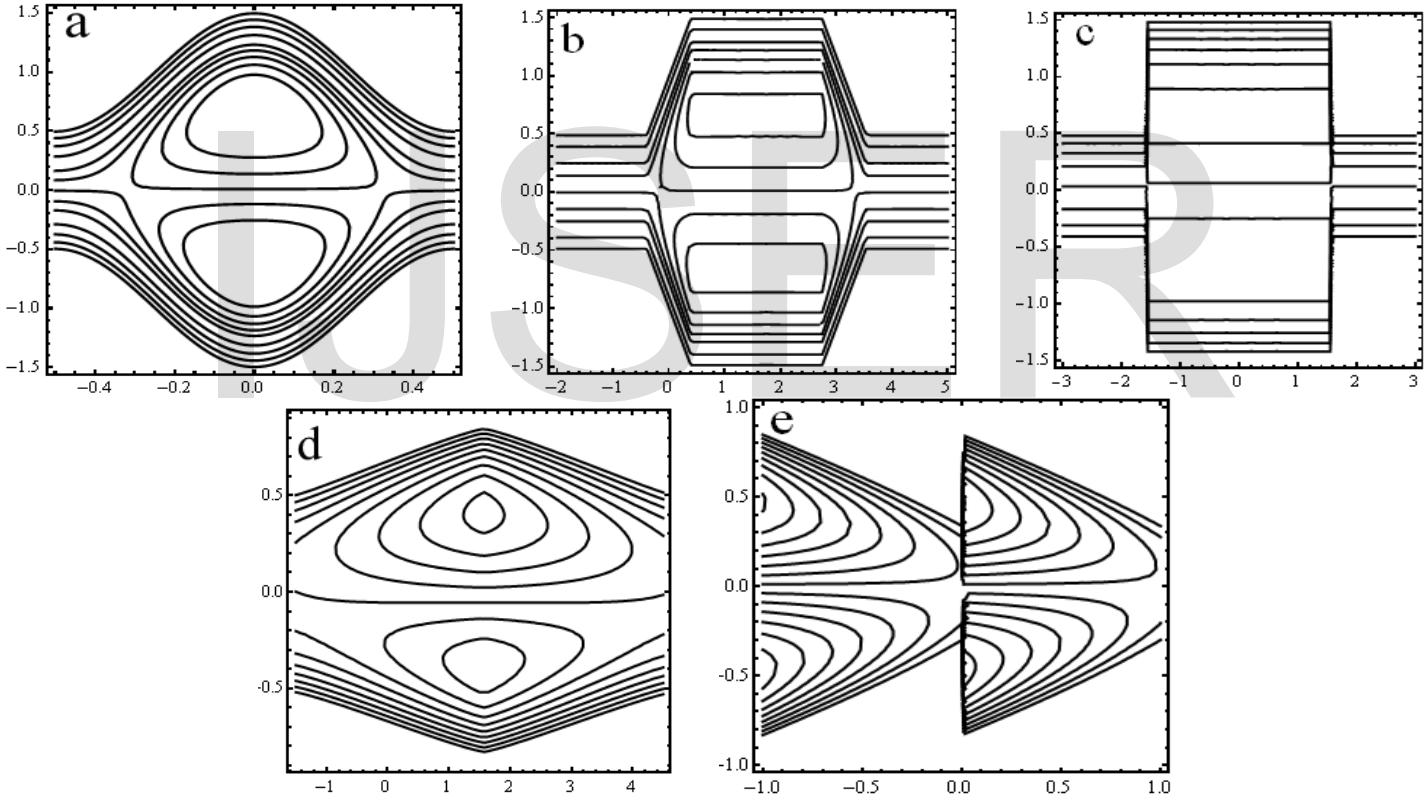


Fig. 10: The stream lines for a=0.5, b=0.5, d=1, $\overline{Q} = 1.5$, $\phi = 0$, n=1, M=1,*We*=0.001; $\beta$=0.01; (a) Sinusoidal; (b) Trapeziodal;(c) Square; (d) Triagle; (e) Sawtooth waves.

than to the Newtonian fluid in upper channel and also an opposite behavior in lower channel.

### 7.1 Trapping phenomena

Another interesting phenomenon in peristaltic motion is the trapping. It is basically the formation of an internally circulating bolus of fluid by closed stream lines. The trapped bolus will be pushed ahead along the peristaltic waves. The stream lines are calculated form Eq. (57) and plotted in Figs. 5-10. Figs. 5 and 7 shows the effects of the volume flow rate $\overline{Q}$ and Weissenberg number $We$ on the stream lines, it is found that the size of the bolus increases with increase $\overline{Q}$ and $We$. It is shown in Figs. 6 that the size of bolus decreases with increasing the Hartmann number $M$ while the bolus disappears for $M$ =3.49. Fig.8 is depicted for various values of the partial slip parameter $\beta$, It is found that the volume of the trapping bolus decreases as the partial slip parameter $\beta$ increases, moreover, the bolus disappears at $\beta$=0.049. Figs. 9-10 compare for different wave forms like sinusoidal, triangular, trapezoidal , square and sawtooth wave, it is finally observed that the volume of trapping bolus of the a Carreau fluid(n=0.398) large in the upper channel and small in the lower channel but an opposite behavior in the case of the Newtonian fluid(n=1).

## Conclusion

We have theoretically analyzed the problem of peristaltic flow of an incompressible MHD Carreau fluid in asymmetric channel under the effect on partial slip with different wave forms. The governing equations are transformed to steady non-dimensional differential equations. These equations are solved analytically. Interaction of various emerging parameters with peristaltic flow is discussed with the help of graphs. On the basis of present analysis, the following observations have been noted:

- The magnitude of the velocity field increases near the walls and decreases at the center of the channel when increasing the Hartmann number $M$ and partial slip parameter $\beta$.
- The pressure gradient decreases with increasing the partial slip parameter $\beta$ and Weissenberg number $We$.
- In the peristaltic pumping region the pressure rise decreases with increasing $We$, $\beta$ In the and $M$ .
- The shear stress distribution decreases in the upper wall and increases in the lower wall of the channel with increasing $M$ and $We$.
- The size of tapping bolus decreases with increase $\beta$ and $M$ while it disappears at $M$ =3.49 and $\beta$=0.06.

## Appendix: Expressions for wave shapes

The non-dimensional expressions for the five considered wave forms are given by the following equations:

I. Sinusoidal wave:

$$h_1(x) = 1 + a\sin(x), \tag{A.1}$$

$$h_2(x) = -d - b\sin(x+\phi), \tag{A.2}$$

II. Triangular wave:

$$h_1(x) = 1 + a\left\{\frac{8}{\pi^3}\sum_{m=1}^{\infty}\frac{(-1)^{m+1}}{(2m-1)^2}\sin[(2m-1)x]\right\}, \tag{A.3}$$

$$h_2(x) = -d - b\left\{\frac{8}{\pi^3}\sum_{m=1}^{\infty}\frac{(-1)^{m+1}}{(2m-1)^2}\sin[(2m-1)x+\phi]\right\}, \tag{A.4}$$

III. Square wave:

$$h_1(x) = 1 + a\left\{\frac{4}{\pi}\sum_{m=1}^{\infty}\frac{(-1)^{m+1}}{(2m-1)}\cos[(2m-1)x]\right\}, \tag{A.5}$$

$$h_2(x) = -d - b\left\{\frac{4}{\pi}\sum_{m=1}^{\infty}\frac{(-1)^{m+1}}{(2m-1)}\cos[(2m-1)x+\phi]\right\}, \tag{A.6}$$

IV. Trapezoidal wave:

$$h_1(x) = 1 + a\left\{\frac{32}{\pi^2}\sum_{m=1}^{\infty}\frac{\sin\frac{\pi}{8}(2m-1)}{(2m-1)^2}\sin[(2m-1)x]\right\}, \tag{A.7}$$

$$h_2(x) = -d - b\left\{\frac{32}{\pi^2}\sum_{m=1}^{\infty}\frac{\sin\frac{\pi}{8}(2m-1)}{(2m-1)^2}\sin[(2m-1)x+\phi]\right\}. \tag{A.8}$$

V. Sawtooth wave:

$$h_1(x) = 1 + a\left\{\frac{8}{\pi^3}\sum_{m=1}^{\infty}\frac{\sin[2m\pi x]}{m}\right\}, \tag{A.9}$$

$$h_2(x) = -d - b\left\{\frac{8}{\pi^3}\sum_{m=1}^{\infty}\frac{\sin[2m\pi x]}{m} + \phi\right\}. \tag{A.10}$$

## References

[1 ] T.W. Latham, Fluid motion in peristaltic pump,M.S.Thesis, MIII, Cambridge, MA,1966.
[ 2] A.M. Siddiqui, W.H. Schehawey, Peristaltic flow of a second-order

fluid in tubes, Journal of Non Newtonian Fluid Mechanics, 53(1994)257–284.

[3] A.H. Shapiro, .Y .Jaffrin, S.L. Weinberg, Peristaltic pumping with long wave length sat low Reynolds number, Journal of Fluid Mechanics, 37(1969) 799–825.

[4] M. Mishra, A. Ramachardra Rao, Peristaltic transport of Newtonian fluid in an asymmetric channel, ZAMP. 54 (2003), 532-550.

[5] M.V. Subba Reddy, A. Ramachandra Rao, S. Sreenadh, Peristaltic motion of a power-law fluid in an asymmetric channel, Int. J. Non-Linear Mech. 42(2007), 1153-1161.

[6] K. Vajravelu, S. Sreenadh, R. Hemadri reddy, K. Murugesan, Peristaltic transport of a Casson fluid in contact with a Newtonian Fluid in a circular Tube with permeable wall, International Journal of Fluid Mechanics Research, Vol. 36(2009)(3), 244-254.

[ 7 ] S. Nadeem, Safia Akram, Heat transfer in a peristaltic flow of MHD fluid with partial slip, Commun Nonlinear Sci Numer Simulat 15(2010), 312–321.

[ 8 ] K. Vajravelu, S. Sreenadh, K. Rajanikanth, Chanhoon Lee, Peristaltic transport of a Williamson fluid in asymmetric channels with permeable walls, Nonlinear Analysis: Real World Applications 13(2012) , 2804-2822

[ 9 ] M. Mishra, A. Ramachandra Rao, Nonlinear and curvature effects on peristaltic flow of a viscous fluid in an asymmetric channel, Acta Mechanica, 168(2004), 35-39.

[10] T. Hayat, Nasir Ali, Zaheer Abbas, Peristaltic flow of a mocropolar fluid in a channel with different wave forms, Phys. Lett, A, 370 (2008), 331-344.

[11] L. M. Srivastava, V. P. Srivastava, Peristaltic transport of blood: Casson model II, J. Fluid. Mech. 122(1984), 439-465.

[12] T. Hayat, S. Noreen, Peristaltic transport of fourth grade fluid with heat transfer and induced magnetic field, ComptesRendusMécanique338(2010) 518–528.

[13] Kh. S. Mekheimer, Effect of magnetic field on peristaltic flow of a couple stress fluid, Phys. Lett. A 371(2008), 4271-4278.

[14] S. Srinivas, R. Gayathri, M. Kothandapani, The influence of slip conditions, wall properties and heat transfer on MHD peristaltic transport, Computer Physics Communications 180(2009)2115–2122.

[15] A.M. Abd-Alla, G.A. Yahya, S.R. Mahmoud, H.S. Alosaimi, Effect of the rotation, magnetic field and initial stress on peristaltic motion of micropolar fluid, Meccanica 47(2012)1455–1465.

[16] A. Ebaid, Effects of magnetic field and wall slip condition on the peristaltic transport of a Newtonian fluid in asymmetric channel, Physics letters A 372(2008) 4493-4499.

[17] S. Srinivas, M. Kothandapani, The influence of heat and mass transfer of MHD peristaltic flow through a porous space with complaints walls, Applied Mathematics and Computation 213 (2009)197- 208

[18] S. Nadeem, S. Akram, Heat transfer in a peristaltic flow of MHD fluid with partial slip, Communications in Nonlinear Science and Numerical Simulation 15 (2010) 312 – 321.

[19] K. Rajanikanth, S. Sreenadh, Y. Rajesh yadav, and A. Ebaid, MHD Peristaltic flow of a Jeffrey fluid in an asymmetric channel with partial slip, Advances in applied Science Research, 2012, 3(6) 3755-3765

[20] Prasana Hariharan, V. Seshadri, Rupak K. Banerjee, Peristaltic transport of non-Newtonian fluid in a diverging tube with different wave forms, Mathematical and Computer Modeling**,** 48(2008)998-1017.

[21] K. Rajnikanth, Y. Rajesh yadav, and S.Sreenadh, The Heat Transfer on the Peristaltic Flow of an MHD Fluid in an Inclined Channel in a Porous, International Journal of Fluid Mechanics 5(2) 2013;pp.81-96.

[22] Y Wang, T. Hayat, N. Ali, M. Oberlack, Magnetohydrodynamics peristaltic motion of Sisko fluid in a symmetric or asymmetric channel. Physica A 387(2008), 347-362.

[23] M. Kothandapani, S. Srinivas, Peristaltic transport of a Jeffrey fluid under the effect of magnetic field in an asymmetric channel. Int. J Non-linear Mech.43 (2008), 915-924.

[24] T. Hayat, Niaz Ahmad, N. Ali, Effects of an endoscope and magnetic field on the peristalsis involving Jeffrey fluid, Communications in Nonlinear Science and Numerical Simulation 13 (2008), 1581–1591.

[25] K. Rajanikanth, S. Sreenadh and A. Ebaid, Peristaltic flow of a in an asymmetric channel with partial slip**,**International Journal of Engineering Sciences & Research Technology**,** 3(2) (2014) 2277-9655